

Geophysical Research Letters®



RESEARCH LETTER

10.1029/2024GL109602

Key Points:

- The charge structure of the TP thunderstorm evolves from an initial inverted dipole to a mature stage tripole with a strong LPCC
- Horizontally distributed negative charge zones from cell merger are simultaneously involved in the discharge of a single lightning flash
- Differences in the relative magnitude of LPCC leads to various types of lightning discharges

Correspondence to:

X. Qie,
qix@mail.iap.ac.cn






Citation:

Liu, D., Li, F., Qie, X., Sun, Z., Wang, Y., Yuan, S., et al. (2024). Charge structure and lightning discharge in a thunderstorm over the central Tibetan Plateau. *Geophysical Research Letters*, 51, e2024GL109602. <https://doi.org/10.1029/2024GL109602>

Received 26 APR 2024

Accepted 5 AUG 2024

Charge Structure and Lightning Discharge in a Thunderstorm Over the Central Tibetan Plateau

Dongxia Liu¹ , Fengquan Li^{1,2} , Xiushu Qie^{1,3,4} , Zhuling Sun^{1,3} , Yu Wang², Shanfeng Yuan^{1,3} , Chunfa Sun^{1,3,4}, Kexin Zhu^{1,3,4}, Lei Wei^{1,3,4}, Huimin Lyu^{1,3,4}, and Rubin Jiang^{1,3}

¹Key Laboratory of Middle Atmosphere and Global Environment Observation (LAGEO), Institute of Atmospheric Physics, Chinese Academy of Sciences, Beijing, China, ²Wuhan NARI Limited Liability Company, State Grid Electric Power Research Institute, Wuhan, China, ³Key Laboratory of Atmospheric Environment and Extreme Meteorology (Chinese Academy of Sciences), Beijing, China, ⁴College of Earth and Planetary Science, University of Chinese Academy of Science, Beijing, China

Abstract The evolution of charge structure involved in lightning discharge of a thunderstorm over the central Tibetan Plateau is investigated for the first time, based on the data from very high frequency interferometer, radar and sounding. During the developing-mature stage, the TP thunderstorm exhibited a tripolar charge structure evolved from an initial inverted dipole. At the mature stage, a bottom-heavy tripole charge structure is clearly presented, with a strong lower positive charge center (LPCC) at temperatures above -10°C , a middle negative charge region between -30°C and -15°C , and an upper positive charge region at $T < -30^{\circ}\text{C}$. As the LPCC was depleted, the charge structure evolved into a normal tripole with a pocket LPCC. The merging between different convective cells resulted in the formation of two adjacent negative charge regions located directly and obliquely above the LPCC, and horizontally arranged different charge regions were simultaneously involved in the same lightning discharge.

Plain Language Summary Tibetan Plateau thunderstorms usually exhibit special convective structures. Using the data from the accurate lightning VHF interferometer, electric field mill, fast/slow antenna and C-band radar, the evolution of the charge structure of thunderstorms and their influence on lightning discharges are investigated. Our observation for the first time revealed the charge structure evolution of the central-TP thunderstorm which involved in the lightning discharge, exhibiting a bottom heavy tripole charge structure with a large LPCC in the mature stage evolved from an initial inverted dipole and the usual tripole in the dissipating stage of the thunderstorm. Under different magnitudes of the LPCC, different types of lightning discharges including -IC, +IC and -CG flashes were generated, indicating the crucial effects of LPCC on the lightning discharge types.

1. Introduction

The Tibetan Plateau (TP) stands as the highest plateau globally, showcasing distinct geological and climatic characteristics. Thunderstorms occurring in this region manifest unique structural and spatiotemporal features compared to those in low-altitude plains (Qie et al., 2014, 2022; Zheng & Zhang, 2021) and they typically exhibited small size, short duration, lower charging and flash rate (Qie et al., 2000, 2005a; Zhang et al., 2004).

Thunderstorms over the TP usually show special inverted dipole and tripolar charge structure, with a larger-than-usual lower positive charge center (LPCC) at the bottom of the thunderstorm (Qie et al., 2002, 2005a; Qie & Zhang, 2019). Qie et al. (2009) investigated the charge structure of thunderstorms in four TP regions with varying elevations, categorizing them into two types which exhibited tripolar charge structure, distinguished by the presence or absence of the strong LPCC, and found that thunderstorms occurring in the central area of the TP were mainly characterized by the strong LPCC. The charge structure of the thunderstorm in Qinghai-TP region, northeastern verge of the TP, transformed to an inverted dipole to a tripole with strong LPCC, and then transitioned to inverted or normal dipole as the thunderstorm decayed by using three-dimensional Very High Frequency (VHF, 270 MHz) lightning location system (Fan et al., 2018; Li et al., 2017, 2020).

The presence of a stronger LPCC plays a significant role in the lightning discharge behavior (Clarence & Malan, 1957; Qie, Zhang, et al., 2005; Qie, Zhang, et al., 2005). Observation and simulation studies suggest that the presence of an excessive LPCC can prevent the occurrence of negative cloud-to-ground (-CG) discharges by

© 2024. The Author(s).

This is an open access article under the terms of the [Creative Commons Attribution License](#), which permits use, distribution and reproduction in any medium, provided the original work is properly cited.

inhibiting the descent of a negative leader toward the ground, resulting in the potential CG flash being converted into an intra-cloud (IC) flash (Mansell et al., 2010; Nag & Rakov, 2009; Qie, Zhang, et al., 2005, Qie, Zhang, et al., 2005; Tan et al., 2014; Wang et al., 2019).

Previous studies on the TP thunderstorms have focused mainly on its northeastern periphery area, but relatively few have investigated the charge structure and the associated lightning activity in the central interior of the TP thunderstorm (Qie & Zhang, 2019). The evolution of the charge structure of TP thunderstorms and its impact on lightning discharge remains incompletely understood. Comprehensive observations, including accurate lightning location by VHF interferometers, electric field mill, fast/slow antenna, C-band Doppler radar and sounding, have been conducted in the Lhasa area of the central TP since 2019. This study is to investigate the evolutionary characteristics of the charge structure involved in the lightning discharges of the central TP thunderstorm and to explore how the charge structure influences the lightning discharge.

2. Data and Method

2.1. Lightning Observation

The observation was conducted in the Lhasa area of the central TP with an average altitude of approximately 3,650 m, surrounded by high mountains, steep slopes and valleys. The observational site situated at coordinates of 91.0°E and 29.6°N, is equipped with VHF interferometer antennas, fast and slow antennas, and electric field mill. To ensure accurate synchronization, all observation data are synchronized with GPS time.

The VHF interferometer operating at a high sampling rate of 400 MS/s with a bandwidth from 35 to 70 MHz and an antenna baseline from 50 to 100 m, is used to locate lightning events in high spatiotemporal resolution accurately (Li et al., 2021; Sun et al., 2016). The lightning signal from the fast antenna serves as a synchronous trigger for the VHF interferometer.

The elevation angle of lightning radiation sources for CG flashes can be low and closer to zero, whereas that for IC flashes is high based on the VHF interferometer. The fast electric field change waveform is combined to distinguish between lightning types. The transfer of negative charge to ground corresponds to a positive change in the waveform of the surface electric field and the fast electric field.

Furthermore, the location of CG flashes is obtained from the State Grid Lightning Detection Network (SGLDN). The detection efficiency of the CG lightning is 94% and the average location error is 489 m (Shi et al., 2022). Return strokes with positive and negative polarities are defined as + CG and −CG flashes, respectively.

2.2. Meteorological Data

Radar reflectivity is obtained from C-band Doppler radar located in Lhasa city with a coverage radius of 230 km. Nine elevations from 0.5° to 19.5° are scanned every 6 min. The composite radar reflectivity used in this study is interpolated into 0.01° (latitude) × 0.01° (longitude) × 1 km (height), representing the maximum reflectivity at each angle.

The Convective Available Potential Energy (CAPE) and Cloud Base Height (CBH) of the thunderstorm are determined by the sounding data and surface observations obtained from the Lasha Meteorological observation station.

The liquid water path (LWP) at two different times obtained from Clouds and the Earth's Radiant Energy System is used to investigate the evolution of hydrometeors in the thunderstorm.

2.3. The Identification of Charge Structure

Lightning is initiated between charged regions of opposite polarity (Thomas et al., 2001; Williams, 2006; Zheng et al., 2019). Lightning leaders propagate bi-directionally and demonstrate a distinct asymmetry after their initiation, wherein the weak positive leader develops in the negative charge region with a speed of 10^4 – 10^5 ms^{−1} and the strongly negative leader develops in the positive charge region with a speed of 10^5 – 10^6 ms^{−1} (Williams, 2006). Using the azimuth-elevation distribution of lightning channels from the VHF interferometer, the polarity of the lightning discharge can be inferred based on the development speed and channel density of lightning. Subsequently, by employing the concept that lightning leaders propagate in charge regions with

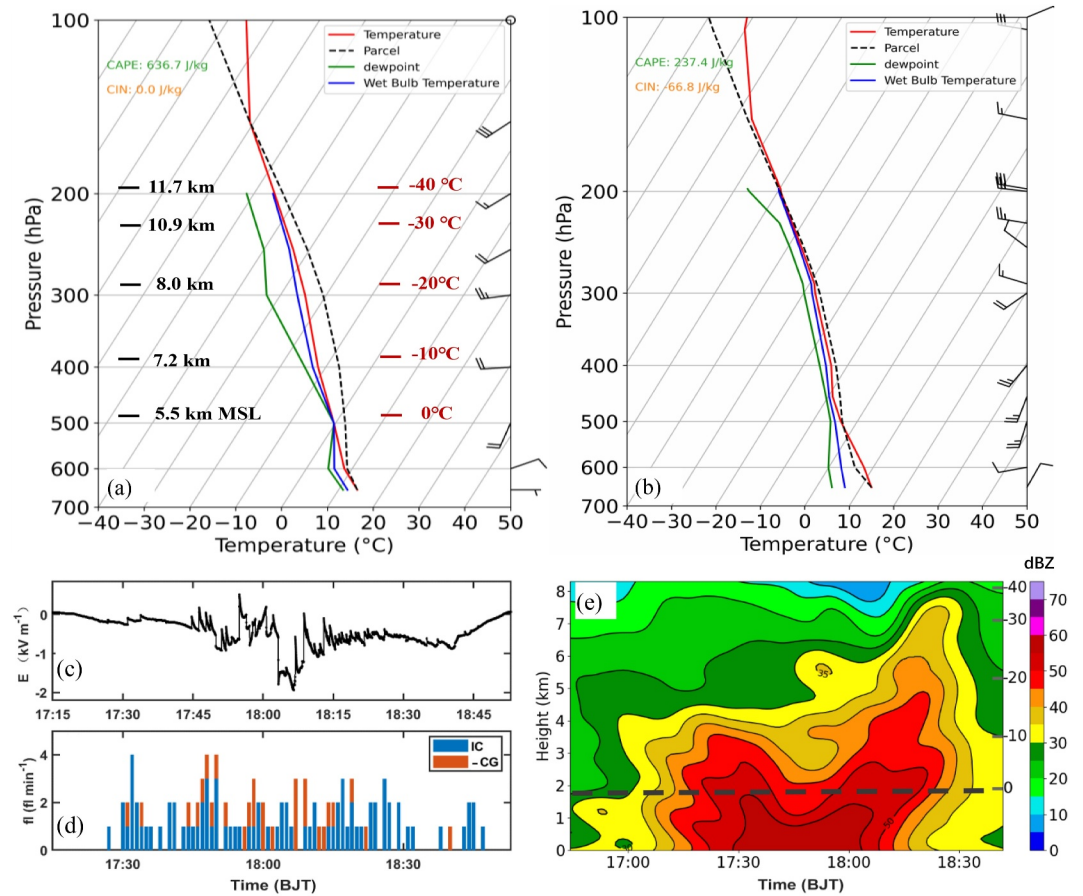


Figure 1. Skew T-logP diagram of the temperature (red line), dew point temperature (green line), the wet bulb temperature (blue line) and parcel temperature observed (a) at 14:00 and (b) 20:00 BJT. Winds are plotted with a full barb 4 m s^{-1} , and half-barb 2 m s^{-1} , black short lines indicate the height (km, MSL) and red short lines represent the in-situ temperature. The temporal electric field (c), the lightning frequency (fl min^{-1}), approximate maximum distance is 10 km away from the center of the thunderstorm. Blue (orange) bar stands for IC (-CG) flashes (d). The time-height of maximum radar reflectivity (e), color shade and black contour stand for radar reflectivity (unit: dBZ), gray dashed line stands for the level of 0°C isotherm, labels on the left-hand axis stand for the height (km, AGL), and the right-hand axis indicate the environmental temperature ($^\circ\text{C}$).

opposite polarity, the charge structure involved in the lightning discharge can be deduced by superimposing in the lightning radiation sources. Although the azimuth-elevation distribution of lightning radiation sources by the VHF interferometer cannot provide the height and distance information, it remains reliable for identifying the charge structure of small-scale thunderstorms during some specific periods by integrating radar observations and environmental temperature.

According to the lightning initiation of IC lightning relative to charge structure, IC flashes can be categorized into negative IC (-IC) and positive IC (+IC) flashes with the -IC flashes occurring between the middle negative and lower positive charge regions (negative dipole), and +IC flashes occurring between the upper positive and middle negative charge regions (positive dipole).

3. Results

A small-size TP thunderstorm occurred on 12 July 2020 within a lifespan of 2 hr. At 14:00, the CAPE reached 637 J/kg and the $0\text{--}6 \text{ km}$ wind shear was 6 m/s (Figure 1a). The CBH was 1 km above ground level (AGL) and the 0°C height was at 1.8 km, together indicating a small warm cloud depth (WCD). It is noted that the thunderstorm developed in a relatively weak environmental condition. The dew point temperature and wet bulb temperature indicated high relative humidity in the air, and facilitated the initiation of convection. The

equilibrium level reached about 9 km (AGL), which corresponded to the low height of convective development over the TP. During the lifetime of the thunderstorm, the surface electric field (Figure 1c) demonstrated mainly negative polarity, indicating a dominated lower positive charge region overhead. Statistical analysis of the fast electric field change (Figure 1d) demonstrated that the maximum lightning frequency reached 4 fl/min, with CG flashes accounting for 25% of total lightning and without + CG flash occurring. During the period of 17:26–18:46 BJT (Beijing Time, the same as below), a total of 84 IC and 29 -CG flashes were detected. As the thunderstorm approached the observational station (17:34 to 18:21), a total of 42 IC and 25 -CG flashes were detected.

The time-height evolution of maximum reflectivity reflects the vertical growth of thunderstorms (Lhermitte & Williams, 1985; Williams et al., 2022). At the initial stage, the radar reflectivity exceeding 35 dBZ is located mainly below the -10°C level (Figure 1e). The vertical development of the thunderstorm is limited to the warmer temperature region. As the TP thunderstorm developed, two distinct pulses in vertical development centered around 17:30 and 18:10, corresponding to an increase in flash rate (Figure 1d). The maximum height of 55 dBZ reflectivity appeared at approximately 2.2 km AGL ($T \approx 0^{\circ}\text{C}$), that of 40 dBZ attained 4 km AGL ($T \approx -15^{\circ}\text{C}$) during the first pulse. With the thunderstorm strengthened and convective cells merged, the maximum reflectivity height of the second pulse experienced a dramatic increase, and suggested the presence of strong updrafts, characterized by the 40dBZ echo heights reaching 6 km AGL ($T \approx -25^{\circ}\text{C}$) with the cloud top extending above 8 km AGL ($T < -40^{\circ}\text{C}$).

As the thunderstorm moved from south to north toward the observation site driven by the southeasterly surface winds, the azimuth of the lightning radiation source underwent rapid and wide-span changes. At the developing-mature stage (17:34), the convection had developed for a while with a maximum radar reflectivity of 50 dBZ at approximately -10°C and 20 dBZ at around -18°C , but no CG flash occurred (Figure 2a). An upper-region + IC and a lower-region -IC flash were detected within the time interval of 13s by the VHF interferometer. The superimposed two IC flashes with the close azimuth and similar estimated distance of lightning discharge indicated the presence of a normal tripolar charge structure involved in the lightning discharge at this stage (Figure 2c).

At 17:45, the thunderstorm entered its mature stage, the convection developed vigorously with the maximum height of 40 dBZ reaching the level of -18°C and the 20 dBZ height extending to -30°C (Figure 2e). The station was located at the northwest edge of the thunderstorm, resulting in a decrease in the azimuth angle of the lightning compared to the situation depicted in Figure 2c. At 17:51, the maximum reflectivity reached 55 dBZ (Figure 2g). During the period of 17:45–17:55, an inverted dipole and a dipole charge structure was retrieved by the superimposed lightning radiation sources. Three -CG flashes were captured by both the SGLDN and the VHF interferometer. Based on the elevation of the lightning and the distance from the return stroke to the observation site, the height of the negative charge region associated with the discharge could be estimated. Considering the potential deviation arising from the lightning horizontal propagation scale of lightning about 10 km, two -CG flashes initiated in the lower charge region with a discharge height of 3.5 ± 0.8 km AGL ($T \approx -10^{\circ}\text{C}$) and one CG flash initiated in the upper charge region with an estimated height of 5.4 ± 1.2 km AGL ($T \approx -23^{\circ}\text{C}$). The analysis of lightning flashes demonstrated a tripolar structure, with the middle negative charge region between around -10°C and -23°C , the upper positive charge region at about $T < -23^{\circ}\text{C}$ and the LPCC at $T > -10^{\circ}\text{C}$ (Figures 2f and 2i). Based on the radiation sources located by the VHF interferometer, it seems that the discharge in the lower dipole of the tripole is more active in this time interval than in the upper dipole.

Two types of -CG flashes were influenced by different positive charge regions of the tripole structure. One type was initiated in the lower inverted dipolar structure, where the negative leader successfully traversed the lower positive charge region to the ground (Figure 2f, black triangles in Figure 2d). The other type contained two -CG flashes initiated in the upper dipolar structure (Figure 2i), where the negative leader traversed the upper positive charge region and developed horizontally before turning toward the ground. At 17:45, one such type of -CG flash occurred in the front flank of the thunderstorm with weak reflectivity of 10 dBZ was found (Figure 2d, black circle). The morphology of the lightning channel indicated that -CG flash originated in the convective region with the negative leader initially developing upwards, shifting to a horizontal trajectory, and eventually propagating downwards to the ground.

From 17:56 to 18:02, the thunderstorm propagated continually northwards with the southerly surface wind (Figure 3a1). The superimposed lightning radiations indicated an inverted dipole (Figure 3e1) and an upper dipole (Figure 3f1) involved in the lightning discharge (with an azimuth of 100°), eventually forming a tripolar charge

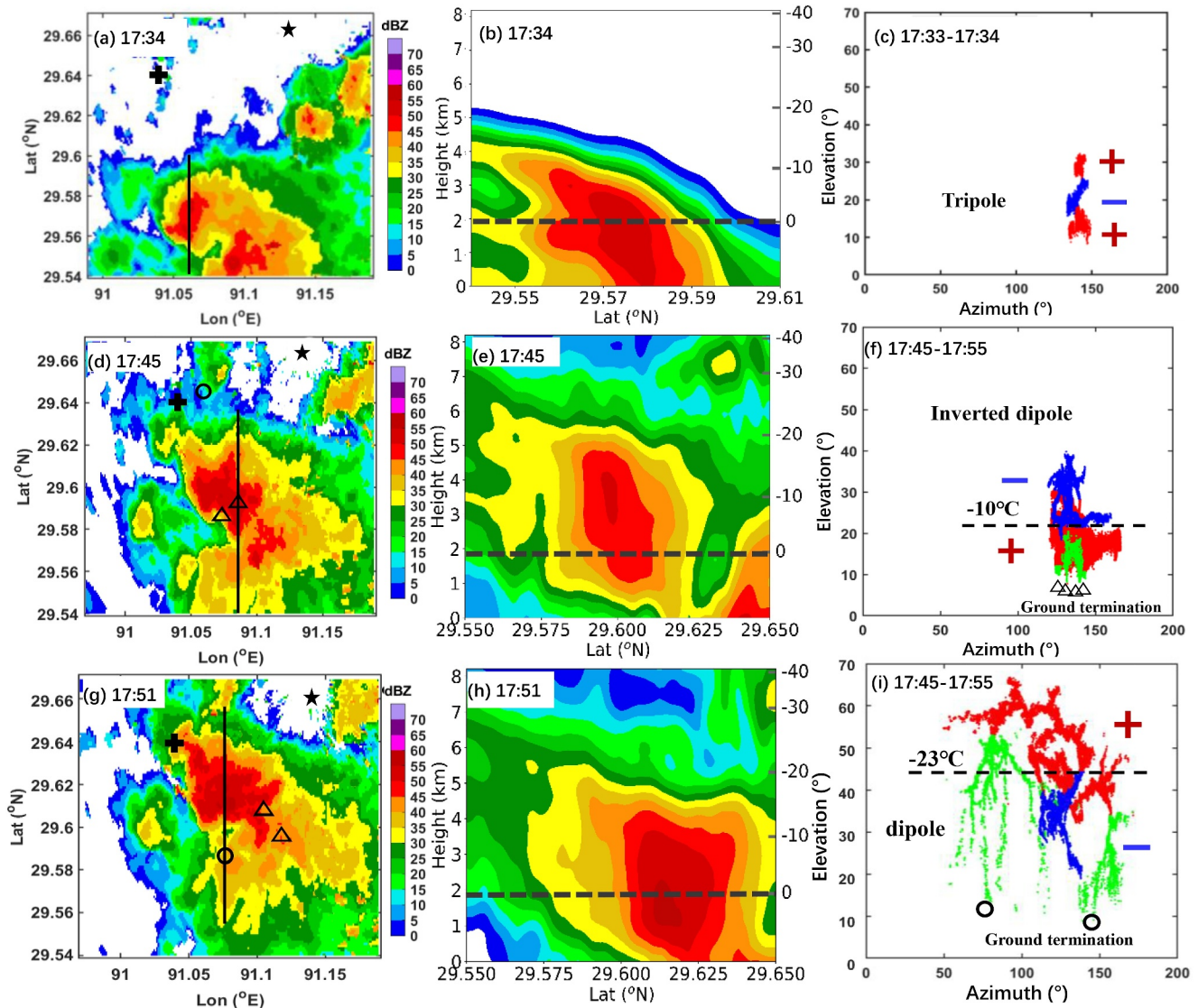


Figure 2. The composited radar reflectivity and the distribution of lightning radiation sources from 17:34 to 17:55 during the developing to mature stage. Composited radar reflectivity superimposed on the CG lightning by the SGLNT at 17:34 (a), 17:45 (d), and 17:51 (g) with the corresponding cross-section of radar echo along the black line (b), (e), (h) with the height and temperature markers, gray dashed lines stand for the level of 0°C isotherm. The superimposed lightning VHF channels by a +IC and (a)IC during 17:33-17:34 (c), five -CG flashes during 17:45 - 17:55 (f). The superimposed lightning channels by 3 +IC flashes and 2 -CG flashes during 17:45-17:55 (i). The red (blue) dots represent the negative (positive) lightning radiation sources, and the green dots represent the negative lightning radiations toward the ground in Figures 2f and 2i. Blue “-” and dark red “+” stand for the negative and positive charge regions, respectively. The black dash line represents the estimated in-situ temperature between two charge regions. The black circles in (d) and (g) represent the ground termination of 2 -CG flashes in Figure 2i. The black triangles represent the ground terminations of 4 -CG flashes in Figures 2d and 2g. Black “+” stands for the observational station, and black star represents the radar site.

structure with a strong LPCC in the convective region. At 17:56, CG flashes were located in radar echo greater than 45 dBZ, with the height of 40 dBZ reaching 5 km AGL ($T \approx -20^\circ\text{C}$) (Figure 3e1). At this time, one CG flash was detected, indicating that the lightning discharge initiated between two charge regions of different polarity at approximately 4.3 ± 0.9 km AGL ($T \approx -15^\circ\text{C}$). In addition, the maximum height of the lightning discharge reached 6.7 km AGL ($T \approx -30^\circ\text{C}$), indicating a 2.4 km AGL depth of the middle negative charge region. At 18:02, the maximum reflectivity reached 50 dBZ and the maximum height of 40 dBZ radar echo extended to 6 km AGL ($T \approx -25^\circ\text{C}$) (Figure 3d1). Two CG flashes were observed, with the lightning discharges initiating at approximately 6.5 km AGL and highest radiation sources appearing at 8.2 km AGL ($T < -40^\circ\text{C}$). Considering the merger process during this period, it is inferred that there may exist two separated negative charge regions involved simultaneously in the lightning discharge, forming a deep-strong negative charge region.

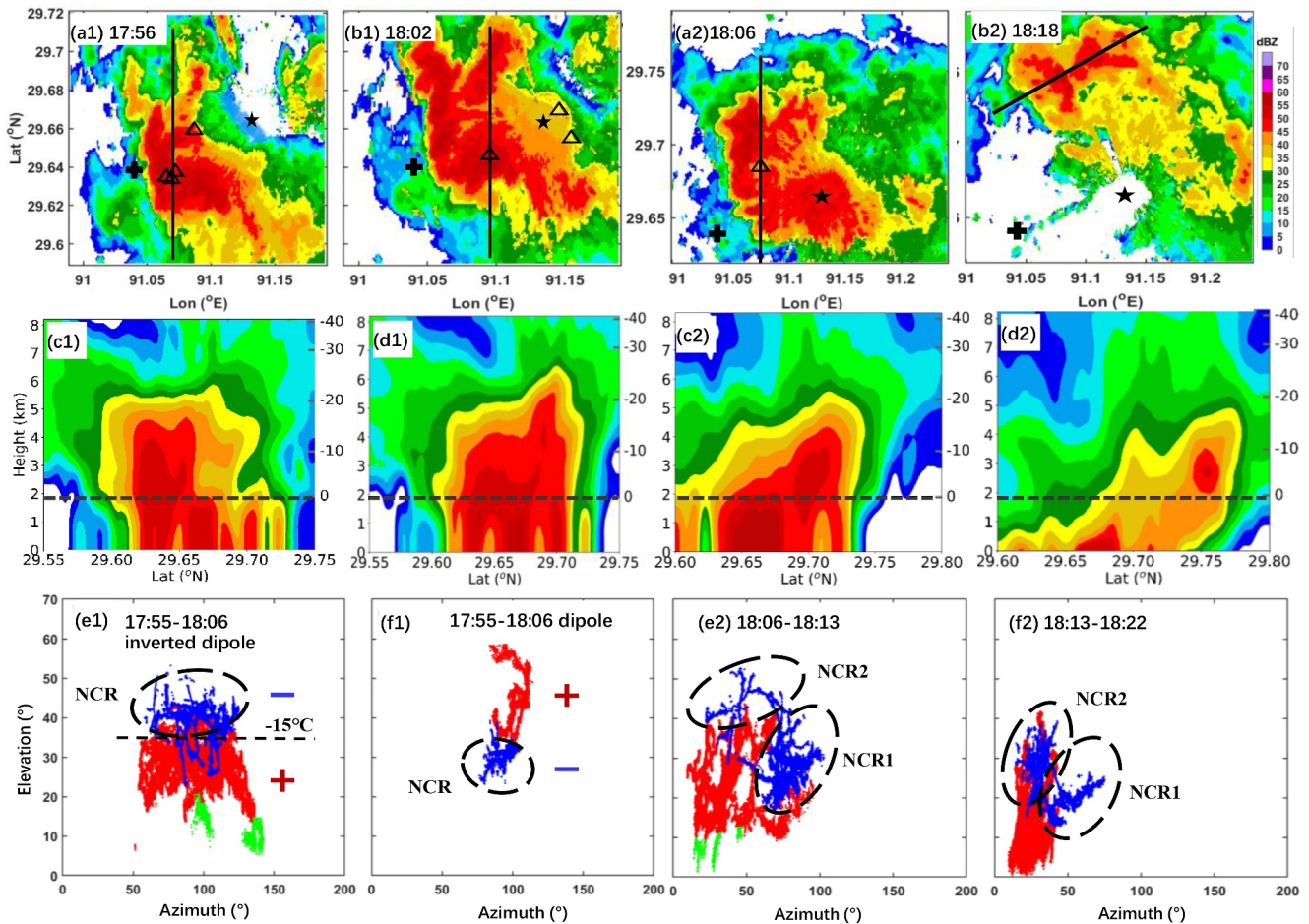


Figure 3. Same as Figure 2 but from 17:56 to 18:13 at the late mature stage, and 18:13 to 18:22 at the dissipating stage (a1) at 17:56 (b1) at 18:02 (a2) at 18:06 (b2) at 18:18, and the corresponded cross-section of radar echo (c1) (d1) (c2) (d2). Lightning radiations for 3 -CG flashes (e1), the lightning channels by 1 -IC flash and 7 -CG flashes from 17:55 to 18:06 (f1), superposition of the lightning channels by 3 +IC flashes (e2). Superimposed by 20 -IC flashes and 1 +IC flash from 18:13 to 18:22 (f2). The black oval dashed line in Figures 3e and 3f stands for the negative charge region (NCR).

At 18:06, corresponding to the late-mature stage, the height of 40 dBZ dropped to 4.5 km AGL with a temperature of about -18°C . The azimuth-elevation diagram depicted six superimposed lightning channels (Figure 3e2), including three -CG and three -IC flashes, indicating that two negative charge regions were involved in the lightning discharge with one located to the lower right of the other. In addition, the large-scale negative charge region (region 1) was located obliquely above the lower positive one, while the small-scale negative charge region (region 2) was placed directly above the lower positive one, probably corresponding to two convective centers. The complexity of the charge structure involved in the lightning discharge is thought to be related to the merging of different convective cells. An adjacent negative charge region was located in the inclined top of the LPCC, in addition to the main body of the thunderstorm that presented a tripolar charge structure (Figure 3c2).

After 18:18, the convection of the TP weakened dramatically with the height of 40 dBZ reflectivity decreasing to -10°C , and the intensity of two convective centers dissipating rapidly. According to the VHF interferometer, only IC flashes occurred during this stage. Additionally, the two diminishing convective centers corresponded to two negative charge regions (Figure 3f2) directly and obliquely above the LPCC, respectively.

4. Discussion and Conclusion

The evolution of the charge structure in a central TP thunderstorm and its influence on the lightning discharge are summarized in Figure 4. At the initial stage, the radar reflectivity exceeding 30 dBZ is located primarily below the level of -15°C . A shallow WCD suppressed the droplet growth resulting in more small droplets being lifted into

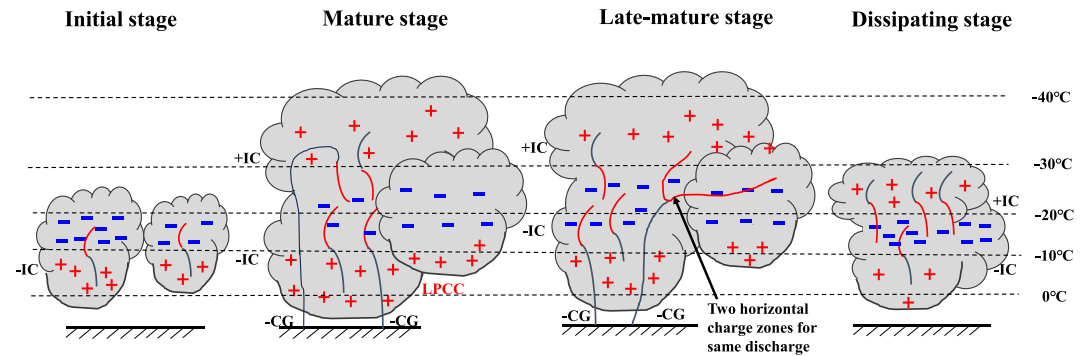


Figure 4. Schematic diagram of the evolution of the charge structure and the different types of lightning discharge. Blue “-” and dark red “+” stand for the negative and positive charge regions, respectively. Red (blue) lines represent the positive (negative) lightning channels and black dashed lines indicate the environmental temperature.

the mixed-phase region to form ice-phase particles such as graupel and ice crystals. Under certain conditions, graupel particles gain positive charge from roughly 0°C to -10°C level in the mixed-phase region. Additionally, the surface electric field showed negative polarity with dominant positive charge region overhead, suggesting the presence of the inverted dipole charge structure at the initial stage (Qie et al., 2005a, 2005b; Bruning et al., 2007; Medina et al., 2022). The positive charge carried by graupel and the negative charge carried by large ice particles (ice crystals and graupel) (Li et al., 2020; Mansell et al., 2010; Qie & Zhang, 2019).

During the mature stage, the maximum height of 40 dBZ and 30 dBZ reached approximately -25°C and -30°C, respectively. The thunderstorm evolved into a tripolar charge structure with a strong LPCC. The main negative charge region extended roughly from -15°C to -30°C, which was mainly responsible for the negatively charged graupel. The inferred large updraft magnitudes favored the appearance and enhancement of the upper positive charge region, which is located around a level of $T < -30^{\circ}\text{C}$ corresponding to small radar reflectivity (<25 dBZ), possibly related to ice crystals or their aggregations. Graupel gained positive charge in the warmer part of the mixed-phase region of the thunderstorm ($T > -10^{\circ}\text{C}$) (Takahashi et al., 2019), contributing to the formation and maintenance of the LPCC. Additionally, the 0°C level of the thunderstorm was around 2 km which facilitated the formation of lower ice particles, playing a critical role in the emergence of LPCC (Qie, Zhang, et al., 2005; Wang et al., 2019). As convective cells merged, an extra adjacent negative charge region formed above the sloping top of the LPCC, creating a deep and broad negative charge region. The strong LPCC and the deep negative charge region contributed to an increased occurrence of -IC flashes, occasionally generating + IC and -CG flashes.

At the late-mature stage, the magnitude of LPCC was gradually weakened due to the positive charge carriers (graupel or hail) converting into liquid drops and falling to the ground. The thunderstorm demonstrated a tripolar charge structure with a main negative charge region between -15°C and -30°C levels, a pronounced upper positive charge region ($T < -30^{\circ}\text{C}$) and a pocket LPCC ($T > -10^{\circ}\text{C}$). Consequently, lightning discharges initiated in the lower inverted dipole structure occurred frequently and the negative leader easily reached the ground from the weak bottom positive charge region, generating more -CG flashes. Moreover, the upper positive charge region and two horizontally displaced negatively charged zones participated simultaneously in the lightning discharge of a single flash, resulting in -CG flashes initiated in the upper dipole charge structure. Therefore, a high-proportion of -CG flashes was influenced by the effect of the lower inverted dipole and the upper dipole of the tripolar charge structure. Additionally, the LWP between the level of 0°C ~ -20°C demonstrated 271 g/m² at 17:30, which indicated a large liquid water content, favoring positively charged graupel at this stage. With the gradual decrease in LWP (14 g/m² at 18:30) in the lower level and the increase ice water path in the upper level, the liquid hydrometeors are gradually converted into ice-phase particles, which contribute to the formation of the main positive dipole of the tripolar charge structure.

As the thunderstorm decayed, the downdraft caused the charge regions to descend to a lower level and the LPCC dispersed. The middle negative charge region was located between -10°C and -20°C levels, with the descent of negatively charged graupel. The upper positive charge region was distributed approximately between the -20°C and -30°C levels, primarily associated with ice crystals and snow. The + IC flash is mainly initiated between the upper positive and middle negative charge region.

Furthermore, the absence of +CG flashes also verified that the deep-broad middle negative region led to sufficient generation of the +IC flashes, thereby preventing the upper positive charge from propagating to the ground. The strong LPCC was not able to initiate + CG flashes either, largely attributed to the possible absence of small negative charge pockets at the bottom below the LPCC and are not conducive to inducing preliminary breakdown processes for the occurrence of +CG flashes (Qie, Zhang, et al., 2005). The TP thunderstorm exhibits the tripolar charge structure with strong LPCC, which differs from the +CG-dominated thunderstorms such as the inverted charge structure (Eddy et al., 2021; Wiens et al., 2005).

Data Availability Statement

This study complies with the AGU data policy. The liquid water path is obtained at <https://ceres.larc.nasa.gov/>. The lightning and radar data examined in this paper are available at Liu (2024).

Acknowledgments

This work was supported by the Second Tibetan Plateau Scientific Expedition and Research (2019QZKK0104), the National Natural Science Foundation of China (Grant 42230609). We thank all those who participated in lightning observation experiments in TP and the Tibetan Meteorological Administrator for their support. We appreciate professor Earle Williams for the constructive suggestions that greatly improved the manuscript.

References

- Bruning, E. C., Rust, W. D., Schuur, T. J., MacGorman, D. R., Krehbiel, P. R., & Rison, W. (2007). Electrical and polarimetric radar observations of a multicell storm in TEXAS. *Monthly Weather Review*, 135(7), 2525–2544. <https://doi.org/10.1175/mwr3421.1>
- Clarence, N. D., & Malan, D. J. (1957). Preliminary discharge processes in lightning flashes to ground. *Quarterly Journal of the Royal Meteorological Society*, 83(356), 161–172. <https://doi.org/10.1002/qj.49708335603>
- Eddy, A. J., MacGorman, D. R., Homeyer, C. R., & Williams, E. (2021). Intraregional comparisons of the near-storm environments of storms dominated by frequent positive versus negative cloud-to-ground flashes. *Earth and Space Science*, 8(5), e2020EA001141. <https://doi.org/10.1029/2020EA001141>
- Fan, X., Zhang, Y., Zhang, G., & Zheng, D. (2018). Lightning characteristics and electric charge structure of a hail-producing thunderstorm on the Eastern Qinghai–Tibetan Plateau. *Atmosphere*, 9(8), 295. <https://doi.org/10.3390/atmos9080295>
- Lhermitte, R., & Williams, E. (1985). Thunderstorm electrification: A case study. *Journal of Geophysical Research*, 90(D4), 6071–6078. <https://doi.org/10.1029/JD090iD04p06071>
- Li, F., Sun, Z., Jiang, R., Tang, G., Liu, M., Li, X., et al. (2021). A rocket-triggered lightning flash containing negative-positive-negative current polarity reversal during its initial stage. *Journal of Geophysical Research*, 126(9), e2020JD033187. <https://doi.org/10.1029/2020JD033187>
- Li, Y., Zhang, G., Wang, Y., Wu, B., & Li, J. (2017). Observation and analysis of electrical structure change and diversity in thunderstorms on the Qinghai-Tibet Plateau. *Atmospheric Research*, 194, 130–141. <https://doi.org/10.1016/j.atmosres.2017.04.031>
- Li, Y., Zhang, G., & Zhang, Y. (2020). Evolution of the charge structure and lightning discharge characteristics of a Qinghai-Tibet Plateau thunderstorm dominated by negative cloud-to-ground flashes. *Journal of Geophysical Research*, 125(5), e2019JD031129. <https://doi.org/10.1029/2019JD031129>
- Liu, D. (2024). Charge structure and lightning discharge in a thunderstorm over the central Tibetan Plateau. [Dataset]. <https://doi.org/10.5281/zenodo.13147375>
- Mansell, E. R., Ziegler, C. L., & Bruning, E. C. (2010). Simulated electrification of a small thunderstorm with two-moment bulk micro-physics. *Journal of the Atmospheric Sciences*, 67(1), 171–194. <https://doi.org/10.1175/2009JAS2965.1>
- Medina, B. L., Carey, L. D., Bitzer, P. M., Lang, T. J., & Deierling, W. (2022). The Relation of environmental conditions with charge structure in central Argentina thunderstorms. *Earth and Space Science*, 9(5), e2021EA002193. <https://doi.org/10.1029/2021EA002193>
- Nag, A., & Rakov, V. A. (2009). Some inferences on the role of lower positive charge region in facilitating different types of lightning. *Geophysical Research Letters*, 36(5), L05815. <https://doi.org/10.1029/2008GL036783>
- Qie, X., Kong, X., Zhang, G., Zhang, T., Yuan, T., Zhou, Y., et al. (2005). The possible charge structure of thunderstorm and lightning discharges in northeastern verge of Qinghai-Tibetan Plateau. *Atmospheric Research*, 76(1–4), 231–246. <https://doi.org/10.1016/j.atmosres.2004.11.034>
- Qie, X., Qie, K., Wei, L., Zhu, K., Sun, Z., Yuan, S., et al. (2022). Significantly increased lightning activity over the Tibetan Plateau and its relation to thunderstorm genesis. *Geophysical Research Letters*, 49(16), e2022GL099894. <https://doi.org/10.1029/2022GL099894>
- Qie, X., Wu, X., Yuan, T., Bian, J., & Lv, D. (2014). Comprehensive pattern of deep convective systems over the Tibetan Plateau–South Asian monsoon region based on TRMM data. *Journal of Climate*, 27(17), 6612–6626. <https://doi.org/10.1175/JCLI-D-14-00076.1>
- Qie, X., Yu, Y., Liu, X., Guo, C., Wang, D., Watanabe, T., & Ushio, T. (2000). Charge analysis on lightning discharges to the ground in Chinese inland plateau (close to Tibet). *Annales Geophysicae*, 18(10), 1340–1348. <https://doi.org/10.1007/s00585-000-1340-z>
- Qie, X., Yu, Y., Wang, H., & Chu, R. (2002). Characteristics of cloud-to-ground lightning in Chinese inland plateau. *Journal of the Meteorological Society of Japan*, 80(4), 745–754. <https://doi.org/10.2151/jmsj.80.745>
- Qie, X., Zhang, T., Chen, C., Zhang, G., Zhang, T., & Wei, W. (2005). The lower positive charge center and its effect on lightning discharges on the Tibetan Plateau. *Geophysical Research Letters*, 32(5), L05814. <https://doi.org/10.1029/2004GL022162>
- Qie, X., Zhang, T., Zhang, G., Zhang, T., & Kong, X. (2009). Electrical characteristics of thunderstorms in different plateau regions of China. *Atmospheric Research*, 91(2–4), 244–249. <https://doi.org/10.1016/j.atmosres.2008.04.014>
- Qie, X., & Zhang, Y. (2019). A review of atmospheric electricity research in China from 2011 to 2018. *Advances in Atmospheric Sciences*, 36(9), 994–1014. <https://doi.org/10.1007/s00376-019-8195-x>
- Shi, T., Yang, Y., Zheng, Z., Tian, Y., Huang, Y., Lu, Y., et al. (2022). Potential urban barrier effect to alter patterns of cloud-to-ground lightning in Beijing metropolis. *Geophysical Research Letters*, 49(21), e2022GL100081. <https://doi.org/10.1029/2022GL100081>
- Sun, Z., Qie, X., Liu, M., Jiang, R., Wang, Z., & Zhang, H. (2016). Characteristics of a negative lightning with multiple-ground terminations observed by a VHF lightning location system. *Journal of Geophysical Research*, 121(1), 413–426. <https://doi.org/10.1002/2015JD023702>
- Takahashi, T., Sugimoto, S., Kawano, T., & Suzuki, K. (2019). Microphysical structure and lightning initiation in Hokuriku winter clouds. *Journal of Geophysical Research*, 124(23), 13156–13158. <https://doi.org/10.1029/2018jd030227>
- Tan, Y. B., Liang, Z. W., Shi, Z., Zhu, J. R., & Guo, X. F. (2014). Numerical simulation of the effect of lower positive charge region in thunderstorms on different types of lightning. *Science China Earth Sciences*, 57(9), 2125–2134. <https://doi.org/10.1007/s11430-014-4867-7>
- Thomas, R. J., Krehbiel, P. R., Rison, W., Hamlin, T., Harlin, J., & Shown, D. (2001). Observations of VHF source power radiated by lightning. *Geophysical Research Letters*, 28(1), 143–146. <https://doi.org/10.1029/2000GL011464>

- Wang, F., Deng, X., Zhang, Y., Li, Y., Zhang, G., Xu, L., & Zheng, D. (2019). Numerical simulation of the formation of a large lower positive charge center in a Tibetan Plateau thunderstorm. *Journal of Geophysical Research*, 124(16), 9561–9593. <https://doi.org/10.1029/2018JD029676>
- Wiens, K. C., Rutledge, S. A., & Tessendorf, S. A. (2005). The 29 June 2000 supercell observed during STEPS. Part II: Lightning and charge structure. *Journal of the Atmospheric Sciences*, 62(12), 4151–4177. <https://doi.org/10.1175/JAS3615.1>
- Williams, E., Mkrtchyan, H., Mailyan, B., Karapetyan, G., & Hovakimyan, S. (2022). Radar diagnosis of the thundercloud electron accelerator. *Journal of Geophysical Research*, 127(11), e2021JD035957. <https://doi.org/10.1029/2021JD035957>
- Williams, E. R. (2006). Problems in lightning physics—The role of polarity asymmetry. *Plasma Sources Science and Technology*, 15(2), S91–S108. <https://doi.org/10.1088/0963-0252/15/2/S12>
- Zhang, Y., Dong, W., Zhao, Y., Zhang, G., Zhang, H., Chen, C., & Zhang, T. (2004). Study of charge structure and radiation characteristic of intracloud discharge in thunderstorms of Qinghai-Tibet Plateau. *Science China Earth Sciences*, 47(z1), 108–114. <https://doi.org/10.1360/04zd0012>
- Zheng, D., Wang, D., Zhang, Y., Wu, T., & Takagi, N. (2019). Charge regions indicated by LMA flashes in Hokuriku's winter thunderstorms. *Journal of Geophysical Research*, 124(13), 7179–7206. <https://doi.org/10.1029/2018JD030060>
- Zheng, D., & Zhang, Y. (2021). New insights into the correlation between lightning flash rate and size in thunderstorms. *Geophysical Research Letters*, 48(24), e2021GL096085. <https://doi.org/10.1029/2021GL096085>